INTERNATIONAL JOURNAL OF ADAPTIVE CONTROL AND SIGNAL PROCESSING
Int. J. Adapt. Control Signal Process. 2009; **23**:808–832
Published online 2 December 2008 in Wiley InterScience (www.interscience.wiley.com). DOI: 10.1002/acs.1100

Set-points reconfiguration in networked multi-area electrical power systems

Alessandro Casavola[1], Domenico Famularo[2], Giuseppe Franzè[1,*,†] and Emanuele Garone[1]

[1]*Dipartimento di Elettronica, Informatica e Sistemistica, Universitá degli Studi della Calabria, Via Pietro Bucci, Cubo 42-C, Rende (CS) 87036, Italy*
[2]*DIMET, Facoltá di Ingegneria, Universitá degli Studi di Reggio Calabria, Reggio Calabria, Via Graziella 89100, Italy*

SUMMARY

In this paper we present a supervisory strategy for load/frequency control problems in networked multi-area electrical power systems. The proposed strategy exploits a recently developed constrained control methodology named *Parameter Governor*, which is based on predictive control ideas and combines in a unique framework the actions of *Reference* and *Offset Governors*. The supervisor reconfigures the nominal frequency set-points and adds offsets to the input terminals of the generation units of each area in order to avoid operative constraint violations when unexpected load changes and/or failures occur. Such a reconfiguration capability is achieved by exploiting the inherent physical redundancy of the power grid and allows, if effective, the enhancement of the overall fault tolerance. The effectiveness of the proposed approach is demonstrated on a two-area power system subject to coordination constraints on maximum frequency deviations, exchanged and generated powers. Copyright © 2008 John Wiley & Sons, Ltd.

Received 3 January 2008; Revised 7 July 2008; Accepted 20 October 2008

KEY WORDS: electric power systems; electrical networks; set-point reconfiguration; command governor; control under constraints

1. INTRODUCTION

Actual multi-area electrical power systems are large-scale and extremely complex interconnected systems. They are composed of generation units, tie-lines and loads organized in a multi-layered hierarchical manner, which exhibit a variety of dynamical behaviors at different time and space scales. A corresponding control framework with many local and some wide-area controllers is

*Correspondence to: Giuseppe Franzè, Dipartimento di Elettronica, Informatica e Sistemistica, Universitá degli Studi della Calabria, Via Pietro Bucci, Cubo 42-C, Rende (CS) 87036, Italy.
†E-mail: franze@deis.unical.it

Contract/grant sponsor: MIUR

required to manage all adverse phenomena such as imbalances, fluctuations, disturbances in a satisfactory way.

Typical local regulation objectives include power system protection, power production stabilization, local voltage and power flow control [1]. These control actions, forming the so-called *primary control layer*, provide basic small-signal compensation and are computed on the basis of local information only. On the contrary, wide-area control actions, which are superimposed to the previously defined local-area actions, are usually referred to as the *secondary control layer* in the power systems jargon. Among them, the load/frequency and the regional voltage control problems are probably the ones mostly considered in literature [2]. As a common feature, they require a regional communication infrastructure to be effective because their actions depend on data spread out in the power grid at far away locations.

Load/frequency control (LFC) has been one of the earlier wide-area control applications proposed in power industry [3–9]. The LFC controller is in charge of keeping the system frequency and the inter-area exchanged power as near as possible to their scheduled values despite changes in load demands. In fact, any imbalance in the generated and consumed power usually leads to frequency deviations that, if too large, have a serious impact on the system operation. Such a situation occurs, as an example, when a generating unit is tripped due to a failure. In such a case, effective LFC strategies would be desirable in order to keep all system variables of interest within acceptable limits during the transients to avoid out-of-services [9].

A lot of papers have addressed this problem from several points of view, e.g. in [6], a robust LFC controller that ensures good performance in the presence of generation rate constraints for a single area has been proposed. A two/four-area power system has been considered in [7], where a solution based on decentralized control ideas was detailed. More recently, a distributed model predictive control framework in conjunction with distributed state estimation strategies has been proposed in [10] for geographically distributed systems such as power systems.

In this paper we propose a tertiary LFC supervisory approach based on constrained predictive control ideas, used recently to synthesize *Reference Governor* (RG) [11–15] and *Parameter Governor* (PG) units [16] in more traditional contexts. The aim is at developing wide-area LFC control schemes for supervising remotely located generation units, connected by distribution lines to remotely distributed loads, under coordination requirements consisting of enforcing pointwise-in-time constraints on the evolutions of relevant system variables. Whenever necessary, in response to unexpected load changes and/or faults, the strategy should be able to reconfigure the nominal set-points on frequency and generated power of each area so that viable evolutions would arise for the overall networked system and a new suitable equilibrium is reached. Notice also that the traditional primary and secondary standard control structures are still present and are not modified by the addition of this proposed tertiary control level.

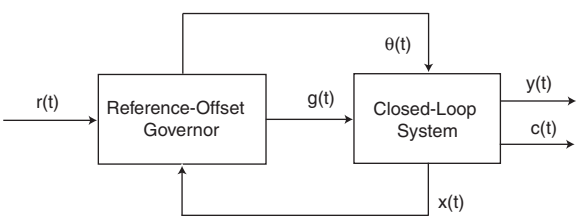

Figure 1. The reference-offset governor (ROG).

DOI: 10.1002/acs

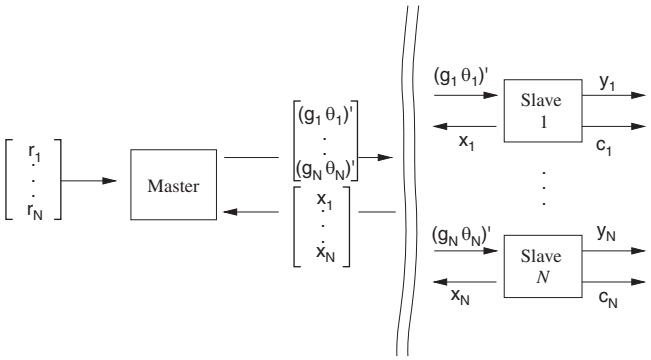

Figure 2. A spatial network of dynamic systems.

The idea is to resort to a general scheme, referred to hereafter as the *Reference-Offset Governor* (ROG) approach. The basic supervisory structure is depicted in Figure 1. There, the ROG unit is an add-on control device superimposed to a primal compensated system, whose action is computed on the basis of the actual reference $r(t)$, the current state $x(t)$ and prescribed constraints $c(t) \in \mathscr{C}$. The aim of the ROG device is to modify, whenever necessary, the reference $r(t)$ into a feasible version $g(t)$ and to generate an offset $\theta(t)$ to be added to the plant input terminal in order to enforce pointwise-in-time constraints on the system transients. The ROG parameters are computed on-line via the minimization of a selection index: the design methodology follows the same lines of RG units described in [11–14] and the PG framework of [16].

In multi-area power systems the supervision and coordination scenario is detailed in Figure 2, where the master is the centralized LFC supervisor and the slaves are the generation units. There, a single master station is in charge of supervising and coordinating several slave systems, which are assumed to be locally compensated dynamical systems equipped with independent sensors, actuators and (semi)-autonomous decision capability. In particular, $r_i, z_i := [g_i \;\; \theta_i]^{\mathrm{T}}$, x_i, y_i and c_i, respectively, represent: the reference, the command (which includes both the reconfigured references and the additional control offsets), the state, performance-related and coordination-related outputs for the ith slave system. In such a context, the supervisory task can be expressed as the requirement of satisfying some tracking performance on y_i, viz. $y_i(t) \approx r_i(t)$, whereas the coordination task consists of enforcing for all times t pointwise-in-time constraints of the form $c_i(t) \in \mathscr{C}_i$ on each slave system and/or $f(c_1(t), c_2(t), \ldots, c_N(t)) \in \mathscr{C}$ on the overall network evolutions.

The paper is organized as follows. In Section 2, a two-area power system model is described and the LFC problem formulated. In Section 3, the ROG unit is discussed and its relevant properties summarized. Section 4 reports simulation results of a detailed investigation undertaken on a two-area power system. Some conclusions finally end the paper.

2. POWER SYSTEM MODEL AND PROBLEM FORMULATION

In this section, a description of a power network and its traditional LFC scheme is presented. For the sake of simplicity, we consider the two-area power system depicted in Figure 3, whose

DOI: 10.1002/acs

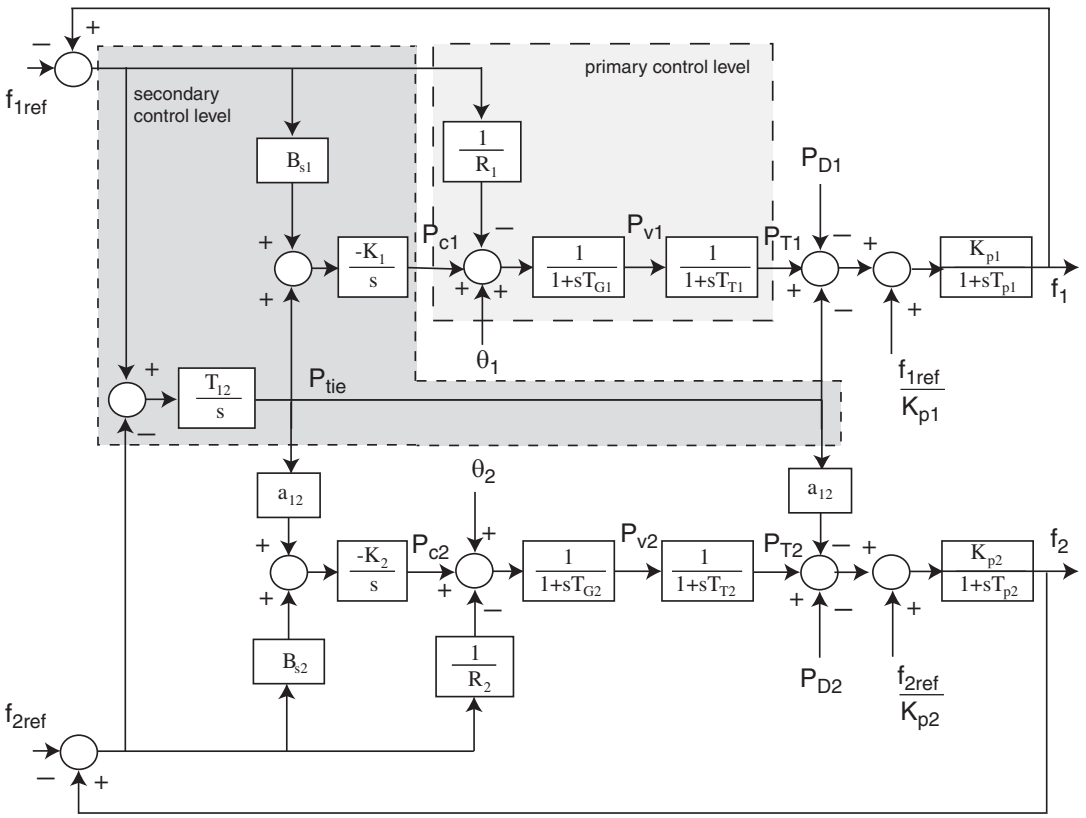

Figure 3. Block diagram of a two-area power system.

small-signal dynamics is described in (1)

$$\begin{aligned}\dot{x}(t) &= Ax(t)+B_1 f_{\text{ref}}(t)+B_2\theta(t)+F(P_D(t)-\xi)\\ y(t) &= Cx(t)\end{aligned} \tag{1}$$

where $f_{\text{ref}}=[f_{1\text{ref}}\ \ f_{2\text{ref}}]^{\text{T}}$, $\theta=[\theta_1\ \ \theta_2]^{\text{T}}$, $y=[y_1\ \ y_2]^{\text{T}}=[f_1\ \ f_2]^{\text{T}}P_D=[P_{D_1}\ \ P_{D_2}]^{\text{T}}$,

$$\xi=\left[\frac{f_{1\text{ref}}}{K_{P_1}}\ \frac{f_{2\text{ref}}}{K_{P_2}}\right]^{\text{T}}$$

and $x=[f_1\ \ P_{T_1}\ \ P_{v_1}\ \ P_{c_1}\ \ P_{\text{tie}}\ \ f_2\ \ P_{T_2}\ \ P_{v_2}P_{c_2}]^{\text{T}}$. The vectors f_{ref} and θ represent, respectively, the frequency set-points and the additional offsets to be added to the nominal control inputs. The constant vector ξ accounts for the representation of the power system LTI model in terms of absolute variables unlike the standard error model used in literature [2, 7]. All other variables are standard and their description can be found in [7].

The task of the primary/secondary control layers is to keep the power system within acceptable operating limits, achieving the load balance $P_T \approx P_D$ and maintaining the area frequencies f_i at their nominal values $f_{i\text{ref}}, i=1,2$. When the power balance prescription is no longer preserved, power losses and frequency deviations usually arise leading to a deteriorated quality of the delivered

DOI: 10.1002/acs

electrical energy and also to the generation of damaging turbine vibrations (at frequencies lower than $\approx$57–58 Hz).

The LFC requirements are traditionally satisfied by the automatic load frequency control (ALFC) stage (primary and secondary loops) included in the scheme (1), which typically takes the form of a proportional-plus-integral local control action. The purpose of the primary loop is to achieve fast adjustments on the produced power P_T in response to frequency deviations. To this end, the speed governor, on the basis of the measured frequency f, produces a command that brings the governor valve P_V and, in turn, the generated power P_T to compensate such deviations. In multi-area power systems, as the one depicted in Figure 3, the secondary ALFC loop is based on an error signal, referred to as the *Area Control Error*, which in addition to frequency deviations also contains information on the exchanged power between the areas via the tie-line [2].

The above ALFC control loop performs in a satisfactory way under small power imbalances arising during normal operating conditions. On the contrary, when the power system falls into an emergency state, e.g. due to a sudden generator loss or to a tie-line disconnection, the ALFC stage is ineffective because turbines exhibit a slow response. In practice, to handle such situations, the power system is equipped with the so-called *emergency control*, whose purpose is to manage abnormal situations and finally to recover the normal operating state. However, such efforts could fail under severe abnormal situations.

Here we define a set of operative and safety constraints to characterize more precisely the *normal conditions* to be imposed. In fact, a tertiary supervisory LFC strategy is used to maintain all evolutions of the power network, originating from load changes and/or faults/failures or other adverse conditions, within the constraints as long as possible by acting on the nominal set-points and on the offset variables. Moreover, the supervisory LFC scheme is demanded to compute a new, possibly dynamic, equilibrium compatible with the changed conditions at a minimum distance from the pre-fault equilibrium.

Hereafter, the following constraints will be considered:

$$f_{\min,i} \leqslant f_i(t) \leqslant f_{\max,i}, \quad i = 1, 2 \tag{2}$$

$$|P_{\text{tie}}(t)| \leqslant \beta_{\max} \tag{3}$$

$$\gamma_{\min,i} \leqslant P_{T_i}(t) \leqslant \gamma_{\max,i}, \quad i = 1, 2 \tag{4}$$

Specifically, constraints (2) prescribe bounds on the maximum frequency deviations for each area, constraint (3) imposes physical bounds on the power flow exchanged between the areas via the tie-line, whereas constraints (4) limit the minimum and maximum suppliable power in each area. The latter constraint comes from the existing limitations on each generation unit, which can be identified as a saturation on the power production.

In what follows, the objective is to show that the action of the proposed tertiary ALFC stage allows one to better cope with critical phenomena in order to avoid, in several cases, the drawbacks related to the traditional ALFC stage. To this end, the next section is devoted to discuss the predictive control architecture of interest here.

3. ROG DESIGN

A ROG control scheme describing the plant, the primal controller (equipped with an integral action) and the ROG device, is depicted in Figure 4. Consider the following linear, time-invariant

DOI: 10.1002/acs

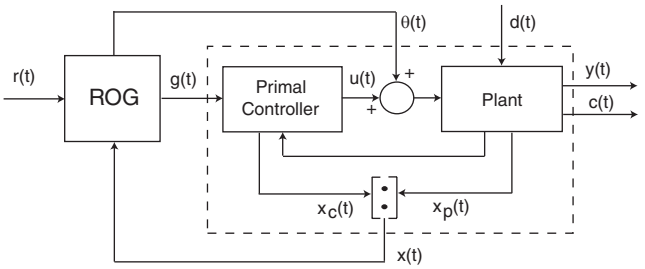

Figure 4. The ROG control scheme.

plant description regulated by the primal controller

$$\begin{aligned} x(t+1) &= \Phi x(t) + G_g g(t) + G_\theta \theta(t) + G_d d(t) \\ y(t) &= H_y x(t) \\ c(t) &= H_c x(t) + L_g g(t) + L_\theta \theta(t) + L_d d(t) \end{aligned} \tag{5}$$

with $x(t) \in \mathbb{R}^n$ the state (which possibly includes the controller states); $g(t) \in \mathbb{R}^m$ the manipulable reference which, if no constraints were present, would essentially coincide with the reference $r(t) \in \mathbb{R}^m$; $\theta(t) \in \mathbb{R}^m$ an adjustable offset on the nominal control input that we assume to belong to a given convex and closed set Θ, with $0_m \in \text{int}(\Theta)$; $d(t) \in \mathbb{R}^{n_d}$ an exogenous bounded disturbance satisfying $d(t) \in \mathscr{D}, \forall t \in \mathscr{Z}_+$ with $\mathscr{D}$ a specified convex and compact set such that $0_{n_d} \in \mathscr{D}$; $y(t) \in \mathbb{R}^m$ the performance-related output and finally $c(t) \in \mathbb{R}^{n_c}$ the constrained vector

$$c(t) \in \mathscr{C} \quad \forall t \in \mathscr{Z}_+ \tag{6}$$

with $\mathscr{C} \subset \mathbb{R}^{n_c}$ being a prescribed convex and compact set. It is assumed that

$$\text{(A1)} \begin{cases} \text{(1) } \Phi \text{ is a stability matrix} \\ \text{(2) The closed-loop system (5) is offset-free i.e.} \\ \quad H_y (I_n - \Phi)^{-1} G_g = I_m \end{cases}$$

Notice that (A1)(1) comes from the fact that (5) represents the closed-loop system while (A1)(2) is considered here only for ensuring offset-free properties to the regulated system, it is not dictated by any technical reason and it happens to be satisfied under a unity feedback configuration with infinity dc loop gain. In the sequel, the following equivalent state description of (5) will be used:

$$\begin{aligned} x(t+1) &= \Phi x(t) + G z(t) + G_d d(t) \\ y(t) &= H_y x(t) \\ c(t) &= H_c x(t) + L z(t) + L_d d(t) \end{aligned} \tag{7}$$

where

$$z(t) := \begin{bmatrix} g(t) \\ \theta(t) \end{bmatrix} \in \mathbb{R}^{2m}, \quad G = [G_g \;\; G_\theta], \quad L = [L_g \;\; L_\theta]$$

DOI: 10.1002/acs

The ROG design problem consists of generating, at each time instant t, the command $z(t)$ as a memoryless function of the current state $x(t)$ and reference $r(t)$

$$z(t) := \underline{z}(x(t), r(t)) \tag{8}$$

in such a way that, under suitable conditions, the constraints (6) are fulfilled for all possible disturbance sequences $d(t) \in \mathscr{D}$ and possibly $y(t) \approx r(t)$ is achieved.

Moreover, it is required that:

(1) $g(t) \to \hat{r}$ whenever $r(t) \to r$, with $\hat{r}$ the best feasible approximation of r and $\theta(t) \to 0_m$;
(2) the ROG has a finite settling time, viz. $g(t) = \hat{r}$ and $\theta(t) = 0_m$ for a possibly large but finite t whenever the reference stays constant after a finite time.

By means of linearity, it is possible to separate the effects of the initial conditions and inputs from those of the disturbances, e.g. $x(t) = \overline{x}(t) + \tilde{x}(t)$, where $\overline{x}(t)$ is the disturbance-free component and $\tilde{x}(t)$ depends only on the disturbances. Then, we adopt the following notations

$$\begin{aligned} \overline{x}_z &:= (I_n - \Phi)^{-1} G z \\ \overline{y}_z &:= H_y (I_n - \Phi)^{-1} G z \\ \overline{c}_z &:= H_c (I_n - \Phi)^{-1} G z + L z \end{aligned} \tag{9}$$

for the disturbance-free equilibrium solutions of (5) to a constant command $z(t) = z$. Consider next the following set recursion

$$\begin{aligned} \mathscr{C}_0 &:= \mathscr{C} \sim L_d \mathscr{D} \\ \mathscr{C}_k &:= \mathscr{C}_{k-1} \sim H_c \Phi^{k-1} G_d \mathscr{D} \\ &\vdots \\ \mathscr{C}_\infty &:= \bigcap_{k=0}^{\infty} \mathscr{C}_k \end{aligned} \tag{10}$$

where $\mathscr{A} \sim \mathscr{E}$ is defined as $\{a \in \mathscr{A} : a + e \in \mathscr{A}, \forall e \in \mathscr{E}\}$. It can be shown that the sets $\mathscr{C}_k$ are non-conservative restrictions of $\mathscr{C}$ such that $\overline{c}(t) \in \mathscr{C}_\infty, \forall t \in \mathscr{Z}_+$, implies that $c(t) \in \mathscr{C}, \forall t \in \mathscr{Z}_+$. Thus, one can consider only disturbance-free evolutions of the system and adopt a 'worst-case' approach. For reasons which have been clarified in [12], it is convenient to introduce the following sets for a given $\delta > 0$

$$\mathscr{C}^\delta := \mathscr{C}_\infty \sim \mathscr{B}_\delta \tag{11}$$

$$\mathscr{W}_\delta := \{z \in \mathbb{R}^{2m} : \overline{c}_z \in \mathscr{C}^\delta\} \tag{12}$$

where $\mathscr{B}_\delta$ is a ball of radius δ centered at the origin and $\mathscr{W}_\delta$ denotes the set of all constant commands whose corresponding steady-state disturbance free constraint variables satisfy the prescribed bounds with a margin δ. Let us assume that there exists a possibly vanishing $\delta > 0$ such that $\mathscr{W}_\delta$ is non-empty. From the foregoing definitions and assumptions, it follows that $\mathscr{W}_\delta$ is closed and convex.

The main idea here is to choose at each time step a constant virtual vector $z(\cdot) \equiv z$, with $z \in \mathscr{W}_\delta$ such that the corresponding virtual evolution fulfills the constraints over a semi-definite

DOI: 10.1002/acs

horizon; moreover, it is required that the offset on the control law and the discrepancy between the command reference $g(t)$ and the constant reference $r(t)$ is minimal. The ROG commands are applied, a new state is measured and the procedure is repeated. In this context we define the set $\mathscr{V}(x(t))$ as

$$\mathscr{V}(x(t)) = \{z \in \mathscr{W}_\delta : \bar{c}(k, x(t), z) \in \mathscr{C}_k, \forall k \in \mathscr{Z}_+\} \tag{13}$$

where

$$\bar{c}(k, x(t), z) = H_c \left(\Phi^k x(t) + \sum_{i=0}^{k-1} \Phi^{k-i-1} G z \right) + L z \tag{14}$$

is to be understood as the disturbance-free virtual evolution at time k of the constrained vector from the initial condition $x(t)$ at time zero under the constant command $z(\cdot) \equiv z$. As a consequence $\mathscr{V}(x(t)) \subset \mathscr{W}_\delta$, and, if non-empty, it represents the set of all constant virtual sequences in $\mathscr{W}_\delta$ whose evolutions starting from $x(t)$ satisfy the constraints also during transients. It can also be shown that such a set is finitely determined, viz. there exists a positive integer k_0 such that (13) is identically characterizable by restricting $k \in \{0, \ldots, k_0\}$, with k_0 computable off-line as described in [14].

The ROG action is based on the minimization of a cost function subject to the constraints imposed by (13). The cost function has the following form:

$$J(z, r) = \|g - r\|^2_{\Psi_g} + \|\theta\|^2_{\Psi_\theta} \tag{15}$$

where $\Psi_g = \Psi_g^{\mathrm{T}} > 0_m$, $\Psi_\theta = \Psi_\theta^{\mathrm{T}} > 0_m$ and $\|v\|_\Psi := v^{\mathrm{T}} \Psi v$. Thus, at each time $t \in \mathscr{Z}_+$, the ROG action is chosen according to the solution of the following constrained optimization problem:

$$z(t) := \arg \min_{z \in \mathscr{V}(x(t))} J(z, r) \tag{16}$$

The following properties hold true for the above described ROG.

Theorem 1

Consider system (7) along with the ROG selection rule (16). Let assumptions (A1) be fulfilled and $\mathscr{V}(x(0))$ be non-empty. Then:

1. The minimizer in (16) uniquely exists at each $t \in \mathscr{Z}_+$ and can be obtained by solving a convex constrained optimization problem, viz. $\mathscr{V}(x(0))$ non-empty implies $\mathscr{V}(x(t))$ non-empty along the trajectories generated by the ROG command (16).
2. The set $\mathscr{V}(x(t)), \forall x(t) \in \mathbb{R}^n$, is finitely determined, viz. there exists an integer k_0 such that if $\bar{c}(k, x(t), z) \in \mathscr{C}_k, k \in \{0, 1, \ldots, k_0\}$, then $\bar{c}(k, x(t), z) \in \mathscr{C}_k, \forall k \in \mathscr{Z}_+$. Such a *constraint horizon* k_0 can be determined off-line.
3. The constraints are fulfilled for all $t \in \mathscr{Z}_+$.
4. The overall system is asymptotically stable; in particular, whenever $r(t) \equiv r$, $\lim_{t \to \infty} \theta(t) = 0_m$ and $g(t)$ converge either to r or to its best steady-state admissible approximation $\hat{r}$, with

$$\hat{z} := \begin{bmatrix} \hat{r} \\ 0_m \end{bmatrix} := \arg \min_{z \in \mathscr{W}_\delta} J(z, r) \tag{17}$$

   Consequently, by the offset-free condition (A1)(2), $\lim_{t \to +\infty} \bar{y}(t) = \hat{r}$, where $\bar{y}$ is the disturbance-free component of y.

DOI: 10.1002/acs

Proof
The proof of points 1–3. can be determined by following the same arguments used in the standard RG approach [11, 17]. Point 4. addresses the asymptotic stability of the overall system under the ROG action. To this end, assume the reference kept constant, $r(t) \equiv r, \forall t \geqslant t^*$. Consider the following candidate Lyapunov function:

$$V(x(t)) := \min_{z \in \mathscr{V}(x(t))} J(z, r) = J(z(t), r) \tag{18}$$

At time $t+1$, $z(t)$ is an admissible solution for (16). In fact, $z(t) \in \mathscr{V}(x(t+1))$ but not necessarily is the minimizer for $\min_{z \in \mathscr{V}(x(t+1))} J(z, r)$. Then, it follows that

$$V(x(t+1)) = \min_{z \in \mathscr{V}(x(t+1))} J(z, r) \leqslant J(z(t), r) = V(x(t)) \quad \forall t \geqslant t^* \tag{19}$$

Hence, $V(x(t))$ is non-negative and monotonically non-increasing, which implies that

$$\lim_{t \to \infty} [V(x(t)) - V(x(t+1))] = 0$$

and a finite limit exists

$$V(x(\infty)) = \lim_{t \to \infty} [\|g(t) - r\|^2_{\Psi_g} + \|\theta(t)\|^2_{\Psi_\theta}] \geqslant 0 \tag{20}$$

Moreover, one must have $\lim_{t \to \infty} \|\theta(t)\|^2_{\Psi_\theta} = 0$ otherwise a contradiction would result. To this end, suppose that $\lim_{t \to \infty} \|\theta(t)\|^2_{\Psi_\theta} = \theta_{\lim} > 0$, with $\theta_{\lim} > 0$. The idea is to compare the optimal control offset value $\theta^*(t)$ at time t with the alternative solution

$$\hat{\theta}(t) := \theta^*(t) \frac{\theta_{\lim}}{\theta_{\lim} + \varepsilon}$$

Because $0_m \in \operatorname{int} \Theta$, the latter choice is feasible at time t if $\varepsilon > 0$ is sufficiently small and a corresponding lower value for the cost function (15) is obtained with respect to $\theta^*(t)$. In fact, by considering the difference on the costs corresponding to $\hat{z}(t) = [g(t) \;\; \hat{\theta}(t)]^{\mathrm{T}}$ and $z^*(t) = [g(t) \;\; \theta^*(t)]^{\mathrm{T}}$ one has

$$J(\hat{z}(t), r) - J(z^*(t), r) = (\hat{\theta} - \theta^*)^{\mathrm{T}} \Psi_\theta (\hat{\theta} + \theta^*) = -\varepsilon \frac{\|\theta^*\|_{\Psi_\theta}}{(\theta_{\lim} + \varepsilon)^2} (2\theta_{\lim} + \varepsilon)$$

Therefore, if $\theta_{\lim} > 0$ and $\varepsilon > 0$ are sufficiently small, one would obtain

$$J(\hat{z}(t), r) < J(z^*(t), r)$$

which contradicts the assumption that $\theta^*(t)$ is the optimal offset at time t. As a consequence

$$\lim_{t \to \infty} \theta(t) = 0_m \tag{21}$$

and

$$V(x(\infty)) = \lim_{t \to \infty} \|g(t) - r\|_{\Psi_g} \tag{22}$$

DOI: 10.1002/acs

From (22), one can state that $g(t)$ converges to r if $V(x(\infty))=0$ or to its best steady-state admissible approximation $\hat{r}$ if $V(x(\infty))>0$. Moreover, by (21) and the offset-free condition (A1)(2), it results that

$$\lim_{t\to\infty}\bar{y}(t)=\lim_{t\to\infty}g(t)$$

and this ends the proof. □

A more detailed description of the CG/ROG approach and its main properties can be found in [12, 17, 18] and references therein. For CGs approached from different perspectives see [13, 14]. For details on the derivation of the quadratic programming problems underlying the CG/ROG action computation, see [19, 20]. Note finally that the numerical burden of the required on-line computations can be tempered according to the available computing power, ranging from solving on-line convex multidimensional QP optimization problems to consulting look-up tables. See the above references for details.

4. SIMULATIONS

The aim of this section is to analyze the behavior of the supervised networked power system and to verify the capabilities of the proposed tertiary LFC scheme to reconfigure the frequency set-points and control offsets despite large load deviations from nominal conditions and/or occurrence of fault events.

In the numerical simulations, the linear turbine model has been enriched by considering a saturation effect (±0.1 limits) on the rate of change of the produced power (see Figure 5). Such a static nonlinear device has been introduced to take into account practical limitations in the turbine

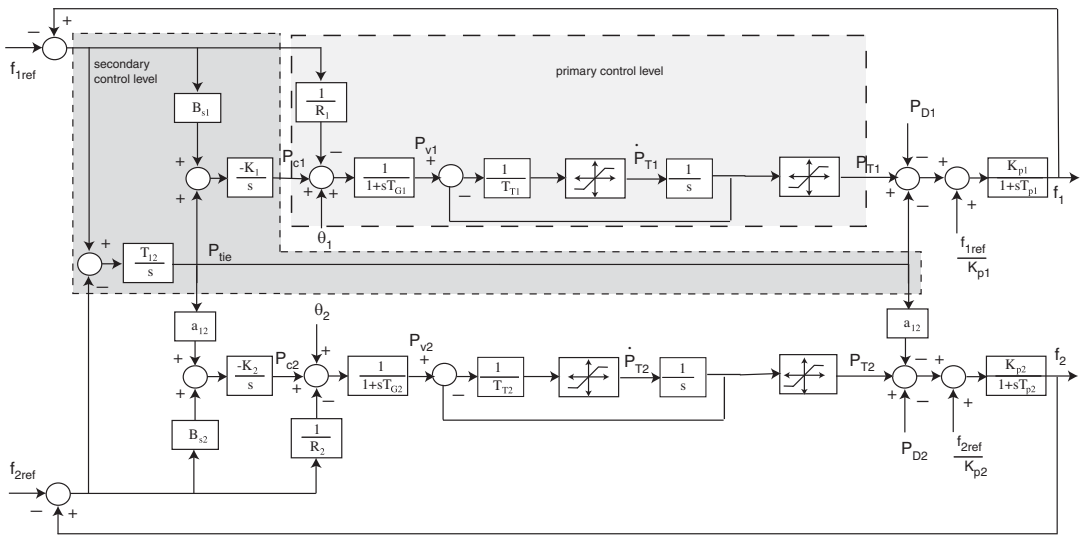

Figure 5. Nonlinear block diagram of a two-area power system.

DOI: 10.1002/acs

response. Moreover, the two-area power system has been also equipped with saturation devices on the produced powers in order to explicitly take into account their physical limits (4).

We consider first the two-area power system with the standard primary and secondary ALFC stages acting as primal controller in the ROG framework. Then, in its linear regime the system (1), along with the constrained variables used in (2)–(4), has been discretized (forward Euler algorithm and sampling period $T_s = 0.1\,\mathrm{s}$) and rewritten as

$$\begin{aligned} x(t+1) &= \Phi x(t) + Gz(t) + G_d(P_D(t) - \xi) \\ y(t) &= H_y x(t) \\ c(t) &= H_c x(t) + Lz(t) + L_d(P_D(t) - \xi) \end{aligned} \tag{23}$$

In (23), $z(t) = [f_{\mathrm{ref}}^{\mathrm{T}}(t) \;\; \theta^{\mathrm{T}}(t)]^{\mathrm{T}}$, $\Phi = \bar{A}$, $G = [\bar{B}_1 \;\; \bar{B}_2]$, $G_d = \bar{F}$ and $H_y = \bar{C}$, with $(\bar{A}, \bar{B}_1, \bar{B}_2, \bar{F}, \bar{C})$ a discrete-time realization of (1). In particular, the following constraint vector:

$$c(t) = [f_1(t) \;\; f_2(t) \;\; P_{\mathrm{tie}}(t) \;\; P_{T_1}(t) \;\; P_{T_2}(t)]^{\mathrm{T}}$$

will be of interest. With this choice, the matrices

$$H_c = \begin{bmatrix} H_y \\ e_5^{\mathrm{T}} \\ e_2^{\mathrm{T}} \\ e_7^{\mathrm{T}} \end{bmatrix}, \quad L_d = 0_{5\times 2}, \quad L = 0_{5\times 4}$$

are used in (23) to exactly characterize the constraints (2)–(4). Note that the vectors $e_i, i = 1, \ldots, 9$, denote the $\mathbb{R}^9$ Euclidean space canonical basis. In all simulations, we have assumed an identical nominal frequency $f_{i\mathrm{ref}}(t) = 60\,\mathrm{Hz}$, $i = 1, 2$, $\forall t$, for each area [9]. The power demand of each area consists of two distinct amounts, $P_{D_i}(t) = \bar{P}_{D_i} + \tilde{P}_{D_i}(t), i = 1, 2$, where $\bar{P}_{D_i} = 3\,\mathrm{MW}$ is a constant load assumed as nominal for both areas and the time-varying amounts $\tilde{P}_{D_i}(t)$, $i = 1, 2$ are used to generate different load variations on each area. It is also worth pointing out that each area has the capability to autonomously balance its own nominal load $\bar{P}_{D_i}$.

Further, in order to properly describe the set of allowable load variations $\tilde{P}_{D_i}$, the following convex and compact region is considered and used in the ROG design:

$$\mathscr{D}_{P_D} := \{\tilde{P}_D \in \mathbb{R}^2 : U\tilde{P}_D \leqslant h\} \tag{24}$$

with $U = \begin{bmatrix} I_2 \\ -I_2 \end{bmatrix}$ and $h = [1, 1, 1, 1]'$[MW]. This choice allows to consider load variations up to $\pm 33\%$ with respect to the nominal value $\bar{P}_{D_i}$ which is a relevant and realistic scenario, as indicated in [21] and references therein. Moreover, the following constraints set (expressed in Hz and MW)

$$\begin{aligned} 58.5 \leqslant f_1(t) \leqslant 61.5, \quad & 58.5 \leqslant f_2(t) \leqslant 61.5 \\ |P_{\mathrm{tie}}(t)| \leqslant 0.48 & \\ 2.2 \leqslant P_{T_1}(t) \leqslant 3.8, \quad & 2.2 \leqslant P_{T_2}(t) \leqslant 3.8 \end{aligned} \tag{25}$$

DOI: 10.1002/acs

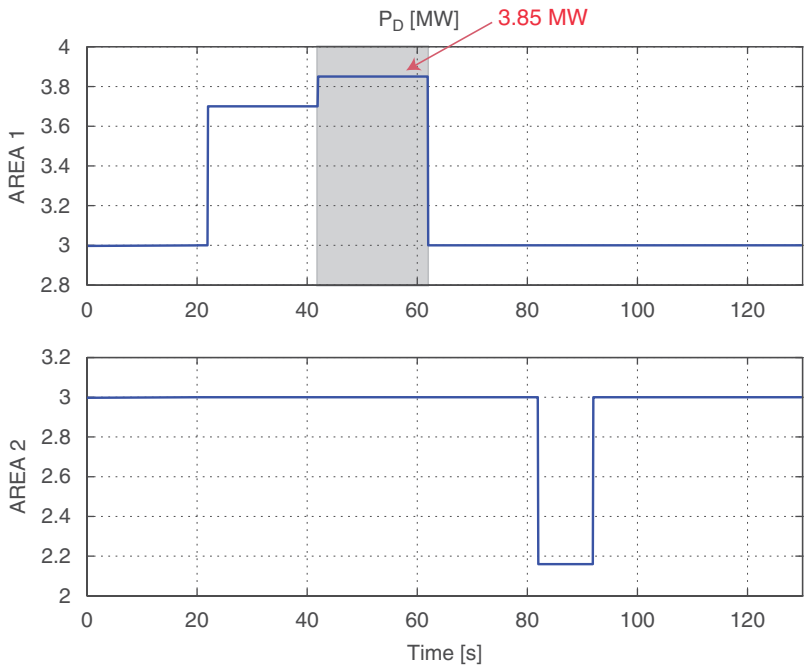

Figure 6. Load demands.

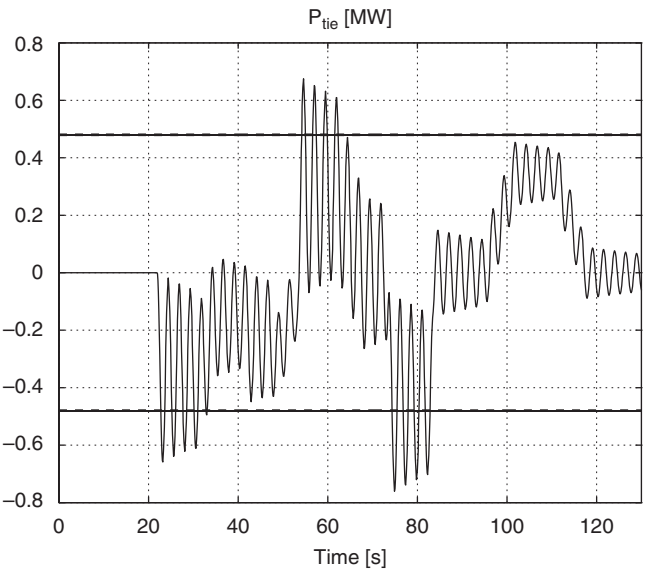

Figure 7. Tie-line power flow: without ROG. The dashed lines represent the boundaries of the prescribed constraint.

DOI: 10.1002/acs

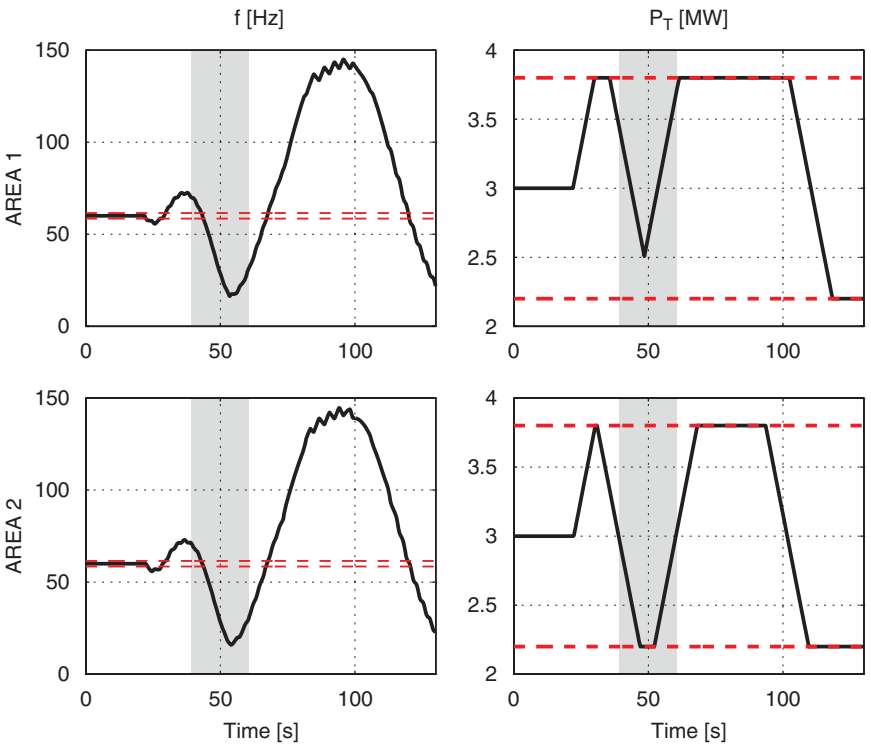

Figure 8. Frequency (left side) and generated power (right side): without ROG. The dashed lines represent the boundaries of the prescribed constraint.

are considered. The starting solution in the ROG design procedure has been imposed equal to $g_i(0) = 60\,\text{Hz}, i = 1, 2$ and $\theta_i(0) = 0, i = 1, 2$, which corresponds to its nominal equilibrium. Some comments on the constraints (25) are mandatory:

- *Frequency deviation*: This is the only constraint that can be freely chosen by the designer. As a general guideline, allowing large frequency deviations it may be of help to guarantee viable system transients as a consequence of large abrupt load changes or faults. The basic idea is that to allow some amount of well-arranged frequency deviations it would produce, under the ROG scheme, lower overshoots and undershoots on all other constrained variables of interest, which therefore may be enforced to stay within their prescribed limits and to avoid the intervention of the tripping devices. We have assumed that the frequency could vary within a range of $\pm 2.5\%$ with respect to its nominal value (60 Hz), which is a quite consistent and effective interval for the above purposes. This choice is also justified by the well-known fact that the frequency drops up to 5% of its nominal value for a power demand change from zero to full load [2, 21].
- *Tie-line saturation*: This constraint is induced by the thermal and surge impedance loading capacity of the transmission line. The first limit is imposed by the capability to withstand the heat generated due to line losses. The other depends on the large inductive reactance of

DOI: 10.1002/acs

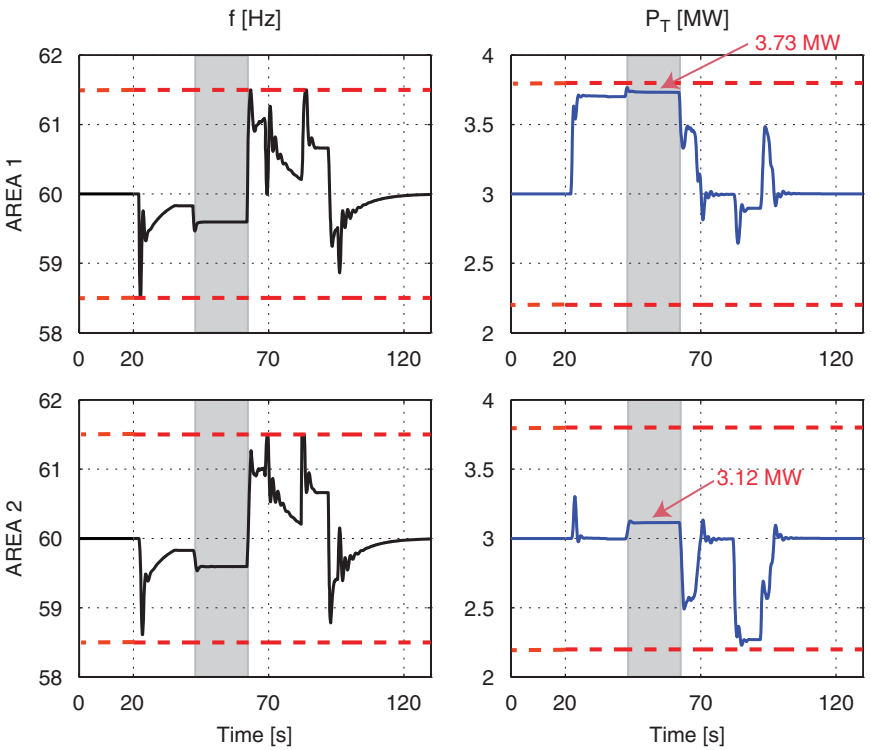

Figure 9. Frequency (left side) and generated power (right side): with ROG. The dashed lines represent the boundaries of the prescribed constraint.

the transmission line that results into large angular separation and voltage drop between two adjacent nodes which may lead to system instability. Here this bound has been considered constant for simplicity although it is and could be considered time varying by adopting a hybrid version of the ROG approach presented here. See [22] for details on hybrid RG approaches. See also [23, 24] for possibilities of DTCR technology in dealing with time-varying tie-line saturation limits.

- *Produced power*: Minimum and maximum levels of power production are usually dictated by physical and economic limitations [9]. Here we have supposed that the maximum allowable power production of each turbine stays within a range of about $\pm 27\%$ w.r.t. its nominal value (3 MW), which is less than the maximum load variation allowed in (24).

The following initial state $x(0) = [60\ 3\ 3\ 3\ 0\ 60\ 3\ 3\ 3]^{\mathrm{T}}$ and ROG parameters $\delta = 10^{-6}$, $\Psi_g = I_2$, and $\Psi_\theta = I_2$ have been chosen. The constraint horizon $k_0 = 300$ was computed via the procedure given in [14]. All simulations have been carried out with MATLAB$^{\mathrm{TM}}$ 7.0 and SIMULINK$^{\mathrm{TM}}$ 6.0.

Three distinct scenarios, each of them representing a relevant and frequent situation leading to power shortages and possibly system breakdowns, will be considered in order to analyze the

DOI: 10.1002/acs

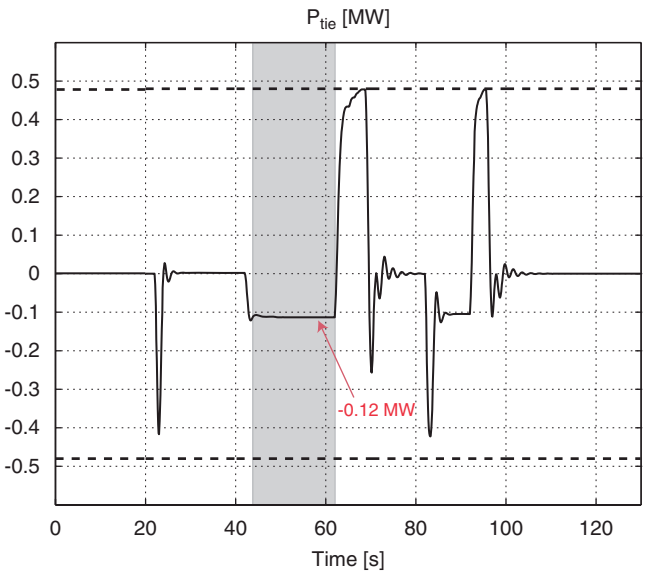

Figure 10. Tie-line power flow: with ROG. The dashed lines represent the boundaries of the prescribed constraint.

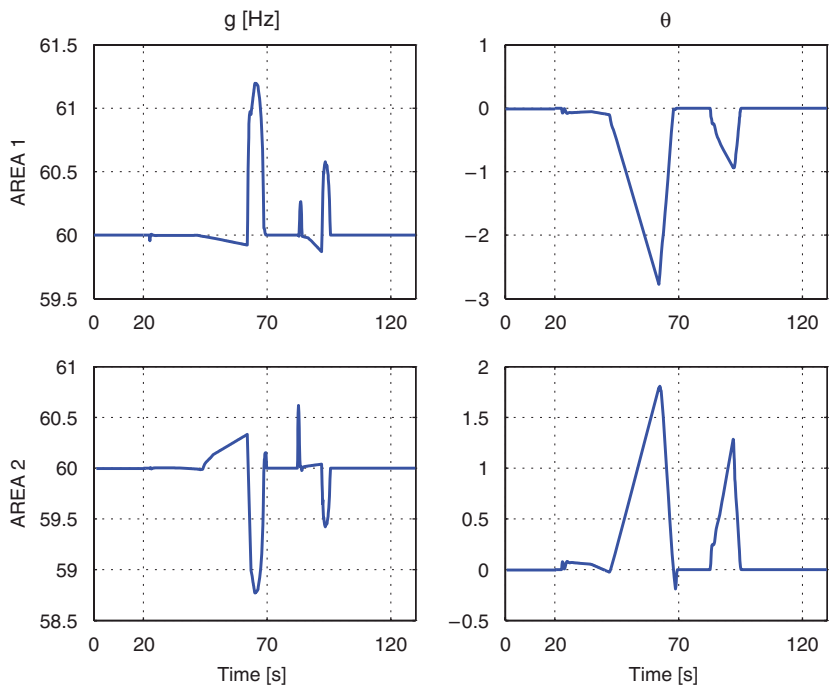

Figure 11. Outputs of the ROG unit. Reconfigured frequency set-points (left side) and control offsets (right side).

DOI: 10.1002/acs

proposed tertiary LFC scheme:

(A) Abrupt load changes (step changes).
(B) Transmission line failure.
(C) Power-generation failure.

The full nonlinear model (Figure 5) will be considered in the simulations. Notice however that the system evolution under the ROG action essentially coincides with that obtained by using a LTI model of the power system. A complete nonlinear model and nonlinear analysis should be used to describe situations related to constraint violations and to the action of protection devices. However, this is outside the scope of this paper, which is in fact mainly focused on how to hold the system evolutions within the prescribed constraints and avoid the intervention of the tripping devices. Anyway, extensions of the ROG approach to nonlinear systems are possible and effective along the lines indicated in [19, 25, 26].

4.1. A-abrupt load changes

The aim of this scenario is to test the effectiveness of the proposed scheme against large load changes. This case can also be regarded as a power contract violation, in the sense that more power than that specified in the contract is temporarily consumed by the customers. On the other hand such a scenario could also be viewed as a consequence of a faulty situation.

Consider the load profiles depicted in Figure 6. There, a load variation in Area 1, followed by a load reduction in Area 2 is assumed. The two variations are not occurring simultaneously

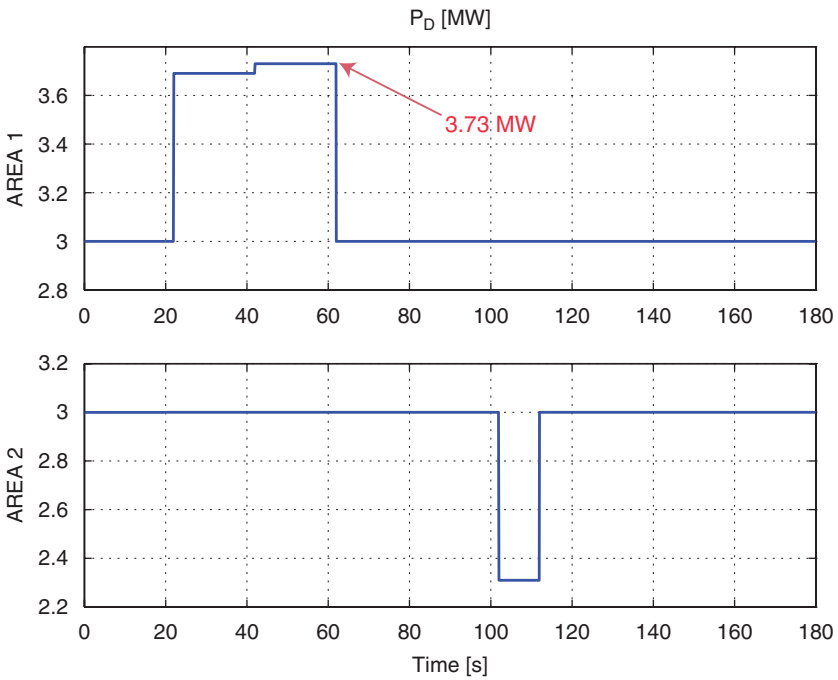

Figure 12. Load demands.

DOI: 10.1002/acs

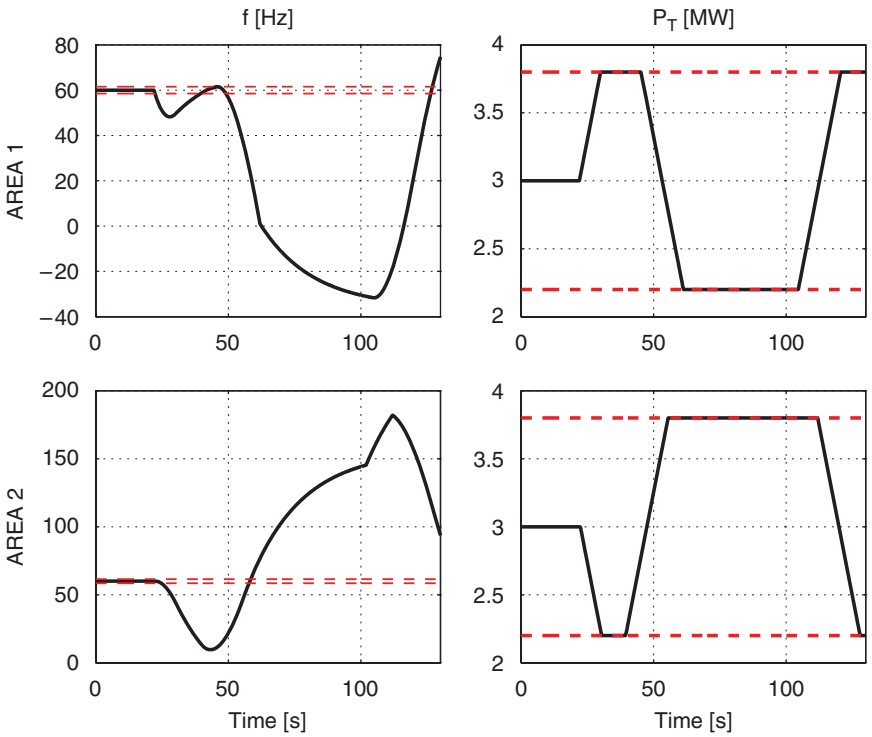

Figure 13. Frequency (left side) and generated power (right side): without ROG. The dashed lines represent the boundaries of the prescribed constraint.

for easiness of presentation. Observe in particular that the Area 1-generation unit is not capable to achieve self-balancing power demand between the time instants $t = 42$ s and $t = 62$ s because it exceeds its limits of a 3.8 MW amount.

Conversely, in Area 2 the load demand (event starting at $t = 82$ s and ending at $t = 92$ s) does not exceed (see the prescribed constraints (25)) its allowable maximum. In principle, such a situation could prevent the matching between production and demand. In order to clarify such a point, let us consider first the behavior of the overall system when only the standard primary/secondary ALFC scheme is used. In Figures 7–8 the evolutions of all constrained variables are reported under the load scenario of Figure 6.

As it clearly results, the standard ALFC is not able to deal with such a critical event. In fact all saturations become active and a power oscillation phenomenon can be observed for the exchanged power in Figure 7 just after the first abrupt load change of 0.69 MW during the time interval $[22, 42]$ s. Observe also how the frequency responses in Figure 8 (left side) overcome the prescribed limits with an increasing unstable trend.

These simulations are of course only indicative because in practice such an unstable behavior is avoided by the intervention of security devices that stops the normal dispatching operations and prevents the occurrence of equipment and infrastructure damages. In particular, when the exchanged power overcomes its physical limits, the opening of a control valve disconnects the

DOI: 10.1002/acs

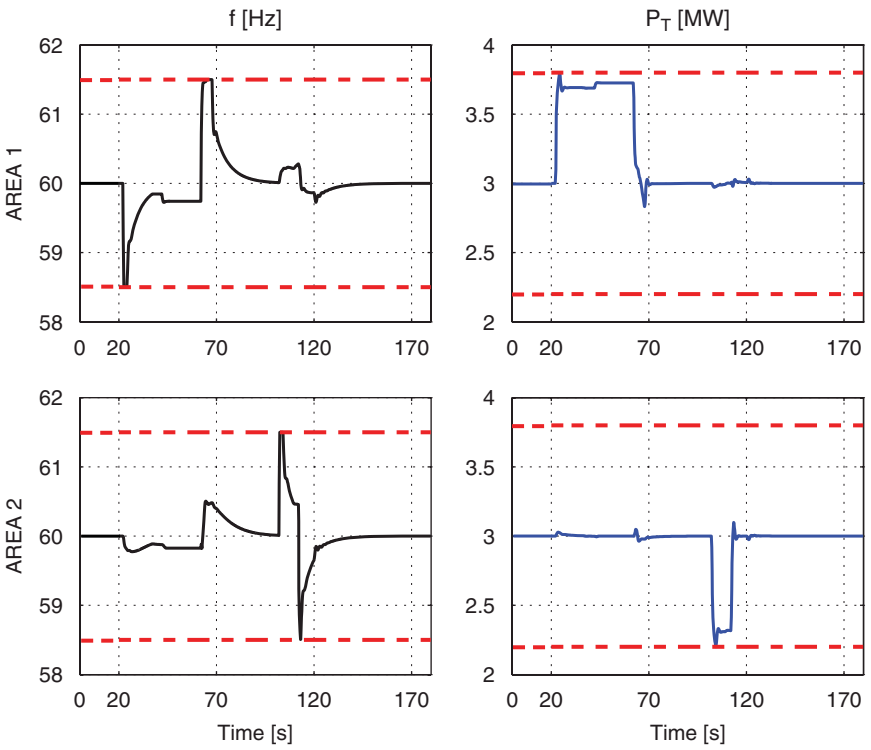

Figure 14. Frequency (left side) and generated power (right side): with ROG. The dashed lines represent the boundaries of the prescribed constraint.

two areas that become, as a consequence, islanded. When this dangerous situation is recovered, the tie-line is reactivated.

This irregular behavior can be avoided if a properly tuned ROG unit is added (see Figures 9 and 10). In fact, observe first that all the variables are always kept inside their bounds and, most importantly, that the ROG device is able to dynamically reconfigure the power balance by modifying the power flows.

In particular, consider the peak demand of 3.85 MW during the gray zone which starts at $t = 42$ s and ends at $t = 62$ s. During this time interval, the ROG unit prescribes a power generation of 3.73 MW for Area 1 in steady-state conditions and the missing power, required to balance the peak load, is obtained from the Area 2 generator (Figure 9), which exactly increases its production of 0.12 MW over its steady-state value. As a consequence, such a fraction is transferred to Area 1 via the tie-line (Figure 10). It must be noted that this new equilibrium has been automatically reached by the ROG unit, which modifies the frequency set-points and adds suitable offsets as depicted in Figure 11. The latter equilibrium results in being the best feasible approximation of the nominal power balance given the changed load conditions. Similar remarks can be made for the load reduction in Area 2. Finally, Figure 11 shows the ROG actions, that is how the set-points and offsets are reconfigured. It is important to note that the control offsets are modified from their nominal values ($\theta_i(0) = 0$, $i = 1, 2$) in order to reduce the frequency deviations.

DOI: 10.1002/acs

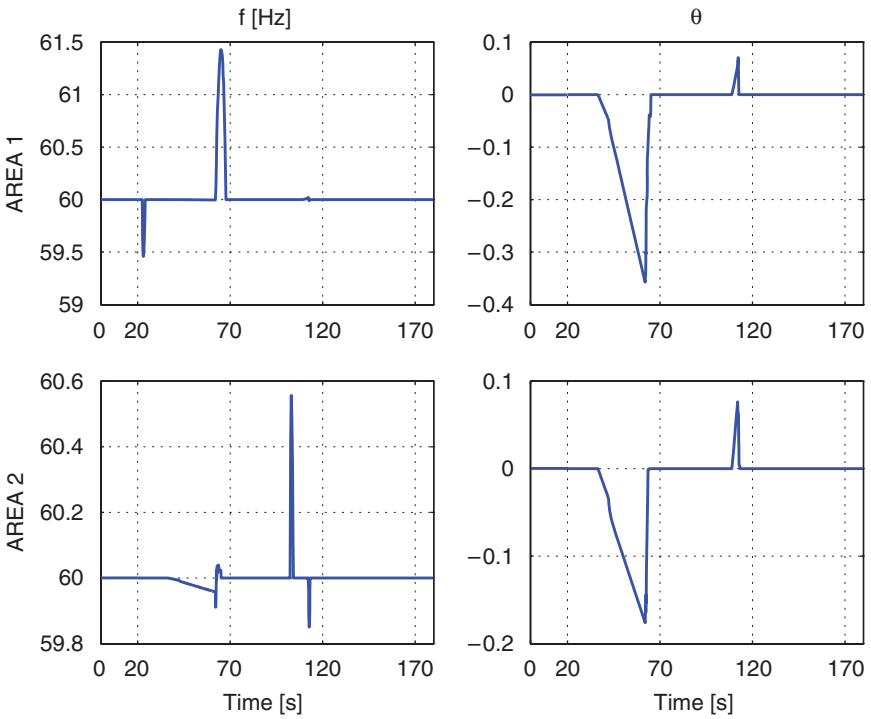

Figure 15. Outputs of the ROG unit. Reconfigured frequency set-points (left side) and control offset (right side).

It is relevant to point out that the fast set point changes in Figure 11 could be quite unrealistic in real power system applications. To this end, it could be more reasonable to enrich the set of constraints by including also rate variation constraints on the variables of interest and on the set-point computation in order to avoid too fast set-point variations.

4.2. B-transmission line failure

In this example we want to investigate how a failure on the transmission line (e.g. power flow breakdown) could affect the whole system evolutions. To this end, the two areas are completely isolated in this example. Notice also that in this faulty case the existence of a solution to the ROG synthesis problem cannot be ensured because the experiment parameters fall outside the sufficient conditions provided by Theorem 1. Nonetheless, even in these unfavorable circumstances, the ROG provides a satisfactory solution in many cases depending on the load profiles and given constraints. The purpose here is to highlight the fault-tolerant properties of the proposed tertiary LFC scheme and its ability at reconfiguring the set-points also in case of faults.

The hypotheses here is that the two areas cannot exchange power due to a failure in the tie-line. When such an event occurs, the two areas lose the possibility of exchanging power. Such a situation implies that the load scenario of the previous experiment (see Figure 6) is not any longer manageable (the ROG problem has not solution), because the power flow between the two areas

DOI: 10.1002/acs

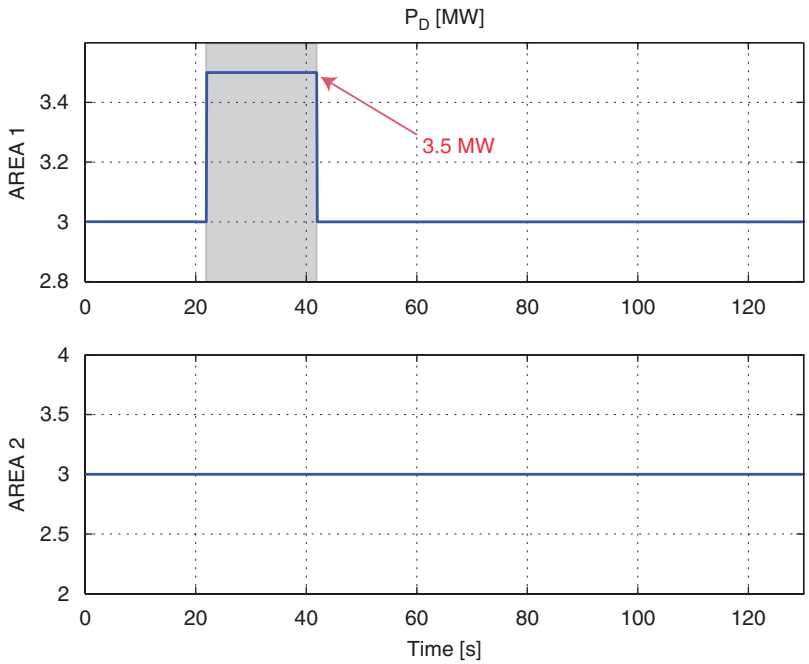

Figure 16. Load demands.

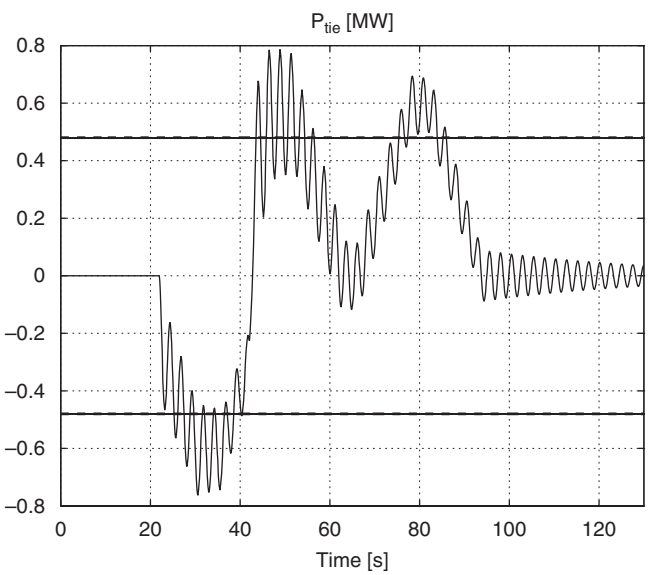

Figure 17. Tie-line power flow: without ROG. The dashed lines represent the boundaries of the prescribed constraint.

DOI: 10.1002/acs

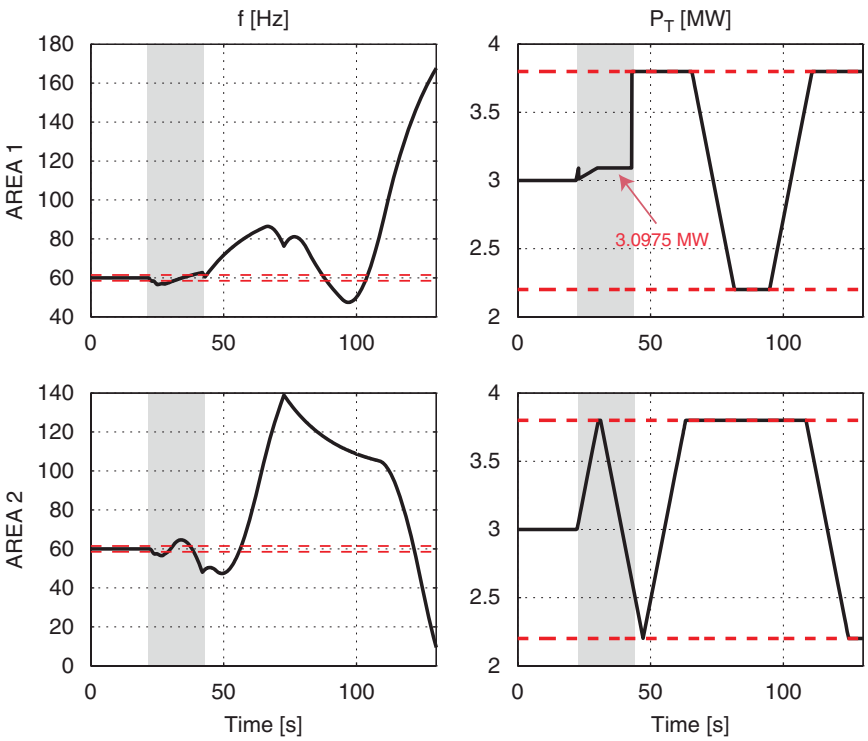

Figure 18. Frequency (left side) and generated power (right side): without ROG. The dashed lines represent the boundaries of the prescribed constraint.

is interrupted and the power balance cannot be achieved. Therefore, we consider the new load demand of Figure 12.

The evolutions of the constrained variables, without and with the ROG unit are, respectively, depicted in Figures 13 and 14. First, observe that when the traditional primary/secondary ALFC scheme is only used, the prescribed constraints are violated (see Figure 13) and again the behaviors show that the overall system evolution remains embedded in a limit cycle.

On the contrary, the ROG insertion allows one to handle this unpredictable event and maintaining the dispatching operativity at the expenses of a degradation of the electrical quality. This is done by suitably modifying the frequency set-points and adjusting the offset parameters as depicted in Figure 15.

4.3. C-power generation failure

This final experiment is instrumental to show the ability of the ROG solution to reallocate the power generation among the areas in the case of generation failures. We shall suppose that a failure occurs on the generator of Area 1 which prevent its capability to autonomously balance the local load.

Specifically, it is assumed that the generator of Area 1 exhibits a 11.5% reduction in its power production from time instants $t=23$ to $t=43$ s due to a fault. This implies that the generator is

DOI: 10.1002/acs

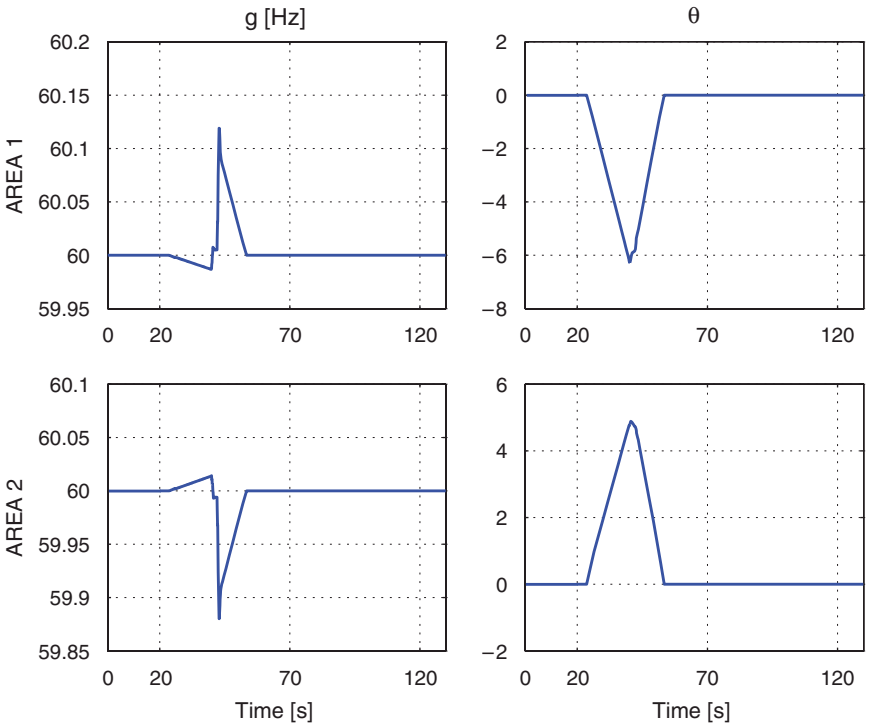

Figure 19. Outputs of the ROG unit. Reconfigured frequency set-points (left side) and control offsets (right side).

capable to provide only 88.5% of its nominal power with respect to the no faulty condition (gain reduction). In addition, a load variation (step change) of 0.5 MW occurs in Area 1 starting at $t = 23$ s and ending at $t = 43$ s, see Figure 16. Note that we have considered that the load disturbance and the power-generation failure occur in the same time interval. Therefore, during the faulty time interval $[23, 43]$ s the Area 1 generator is only capable to produce a maximum of 3.1 MW, as shown in the next Figure 18, and it cannot satisfy the local load demand. Therefore, a new equilibrium has to be determined.

Again, it turns out that the standard primary/secondary ALFC action alone is not capable to cope with such an extreme event. In fact, starting from $t = 23$ s the two area frequencies and their exchanged powers break through their prescribed constraints while the produced powers behavior is like a 'bang-bang' saturated signal (see Figures 17 and 18).

On the contrary, the ROG unit is capable to properly modify the nominal frequency set-points and control offsets (see Figure 19) and to reach a new feasible power balance. In response to this situation, the Area 2 generator increases its power production w.r.t its local demand and the surplus is transferred to Area 1 via the tie-line (Figure 20) so as to compensate the faulty generator (Figure 21).

To better clarify this behavior, consider the time interval $[23, 43]$ s, where the frequencies, the produced and exchanged powers reach new steady-state set-points. In particular, Area 1 produces 3.02 MW, and receives via the tie-line 0.33 MW produced by Area 2. Therefore, a total power

DOI: 10.1002/acs

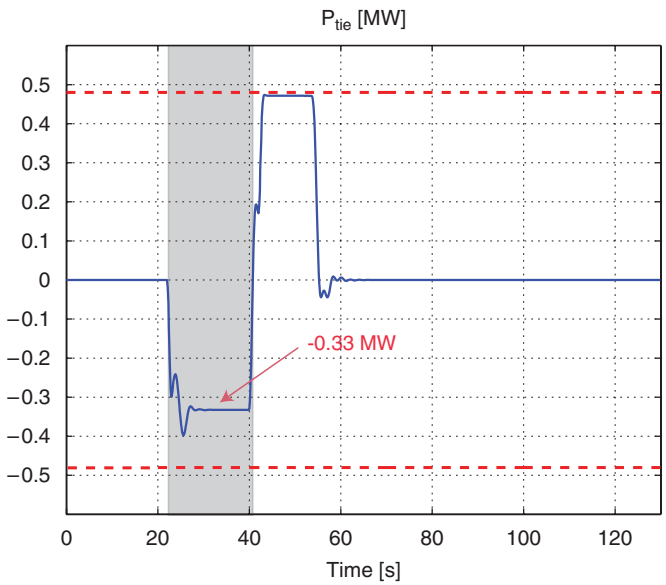

Figure 20. Tie-line power flow: with ROG. The dashed lines represent the boundaries of the prescribed constraint.

amount of 3.35 MW is supplied while the local demand is 3.5 MW instead. This means that, due to generation reduction in Area 1, it is not possible to match the load request. Anyway the ROG automatically reaches the best feasible equilibrium compatible with the failure occurrence. Note also that the operating frequency settles down to 59.0057 Hz in both Area 1 and Area 2. Finally, it is worth commenting that the ROG unit is not informed of the fault occurrence and nonetheless is able to manage such an unpredictable event.

5. CONCLUSIONS

In this paper a supervisory strategy for wide-area LFC control problem has been presented. Details on its effectiveness in coordinating power-generation units and maintaining relevant variables of the grid within prescribed safety constraints have been reported. Special efforts have been devoted at investigating how this class of strategies behave under critical events as faults, failure or abrupt changes in the load demand.

The main feature is the ability to take advantage of the existing physical redundancy (typically in inter-area links and power-generation units) of power grids in order to enhance the fault tolerance capabilities. Pointwise-in-time constraints on frequency deviations, exchanged and generated powers have been considered. Constraints fulfillment is achieved by adjusting an offset on the nominal control law and reconfiguring the frequency set-points.

Relevant examples have been presented where hard-to-predict adverse phenomena have been considered as benchmark problems for the proposed strategy. It has been shown that the standard

DOI: 10.1002/acs

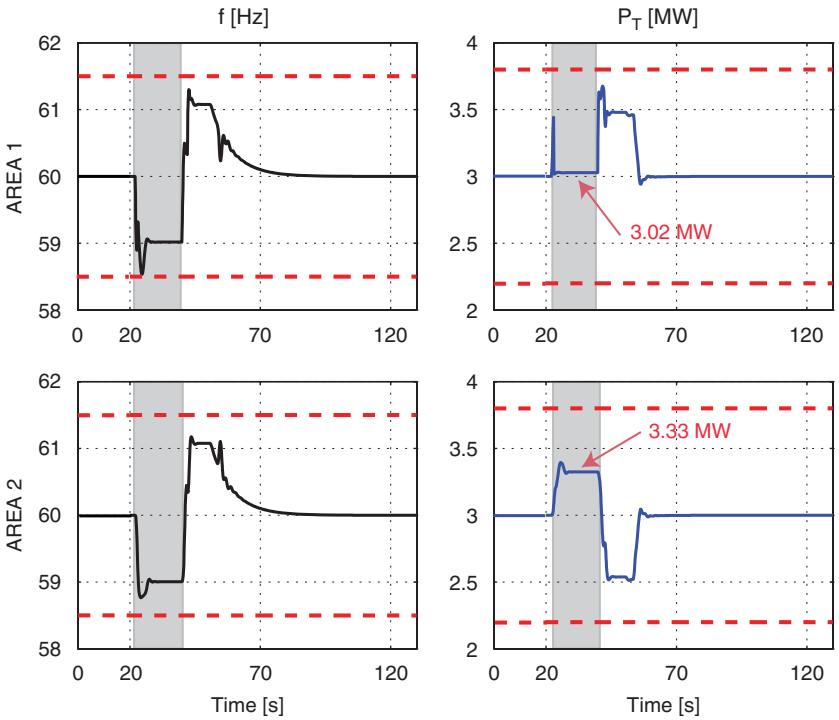

Figure 21. Frequency (left side) and generated power (right side): with ROG. The dashed lines represent the boundaries of the prescribed constraint.

primary/secondary ALFC control schemes are ineffective whereas the proposed tertiary level has been proved to be effective in handling such failure events.

Simulation results have shown encouraging preliminary results in ensuring feasible evolutions of the overall power system with respect to the prescribed operative constraints despite changes in the loads and/or faulty situations under a simplified scenario.

Future works will include the application of the proposed strategy to more realistic situations, with many generation units and tie-lines and delayed or missed pieces of information on the full state of the power system due to communication time-delay and packet drops. In this more general scenario, it seems natural to consider and investigate decentralized or distributed variants of the proposed centralized approach.

ACKNOWLEDGEMENTS

This work has been partially supported by MIUR Project Fault Detection and Diagnosis, Control Reconfiguration and Performance Monitoring in Industrial Process.

REFERENCES

1. Tomsovic K, Bakken DE, Venkatasubramanian V, Bose A. Designing the next generation of real-time control communication and computations for large power systems. *Proceedings of the IEEE* 2005; **93**(5):965–979.

DOI: 10.1002/acs

2. Elgerd OI. Control of electric power systems. *IEEE Control Systems Magazine* 1981; **1**(2):4–16.
3. Nobile E, Bose A, Tomsovic K. Feasibility of a bilateral market for load following. *IEEE Transactions on Power Systems* 2001; **16**:782–787.
4. Bhowmik S, Tomsovic K, Bose A. Communication models for third party load frequency control. *IEEE Transactions on Power Systems* 2004; **19**(1):543–548.
5. Yu X, Tomsovic K. Application of linear matrix inequalities for load frequency control with communication delays. *IEEE Transactions on Power Systems* 2004; **19**(3):1508–1515.
6. Wang Y, Zhou R, Wen C. Robust load-frequency controller for power systems. *IEE Proceedings—C* 1993; **140**(1):11–16.
7. Yang TC, Ding ZT, Yi H. Decentralized power system load frequency control beyond the limit of diagonal dominance. *Electrical Power and Energy Systems* 2002; **24**:173–184.
8. Lim KY, Wang Y, Zhou R. Decentralized robust load-frequency control in coordination with frequency-controllable HVDC links. *Electrical Power and Energy Systems* 1997; **19**(7):423–431.
9. Andersson G. Modelling and analysis of electrical power systems. *Ph.D. Thesis*, Power Systems Laboratory, ETH Zürich, 2004.
10. Venkat AN, Hiskens IA, Rawlings JB, Wright SJ. Distributed MPC strategies for automatic generation control. *Proceedings of the IFAC Symposium on Power Plants and Power Systems Control*, Kananaskis, Canada, vol. 93(5), June 2006.
11. Casavola A, Papini M, Franzè G. Constrained supervision of dynamic systems in spatial networks. *IEEE Transactions on Automatic Control* 2006; **51**(3):421–437.
12. Bemporad A, Casavola A, Mosca E. Nonlinear control of constrained linear systems via predictive reference management. *IEEE Transactions on Automatic Control* 1997; **42**:340–349.
13. Gilbert EG, Kolmanovsky IV, Tin Tan K. Discrete-time reference governors and the nonlinear control of systems with state and control constraints. *International Journal of Robust and Nonlinear Control* 1995; **5**:487–504.
14. Gilbert EG, Tin Tan K. Linear systems with state and control constraints: the theory and applications of maximal output admissible sets. *IEEE Transactions on Automatic Control* 1991; **36**:1008–1020.
15. Bemporad A, Mosca E. Fulfilling hard constraints in uncertain linear systems by reference managing. *Automatica* 1998; **34**:451–461.
16. Kolmanovsky IV, Sun J. Parameter governors for discrete-time nonlinear systems with pointwise-in-time state and control constraints. *Automatica* 2006; **42**(5):841–848.
17. Casavola A, Mosca E, Angeli D. Robust command governors for constrained linear systems. *IEEE Transactions on Automatic Control* 2000; **45**:2071–2077.
18. Casavola A, Mosca E, Papini M. Control under constraints: an application of the command governor approach to an inverted pendulum. *IEEE Transactions on Control Systems Technology* 2004; **12**:193–204.
19. Bemporad A, Casavola A, Mosca E. A predictive reference governor for constrained control systems. *Computers in Industry* 1998; **36**:55–64.
20. Casavola A. The command governor approach for dummies. *DEIS Technical Report 07-2005*, University of Calabria, 2005.
21. Rerkpreedapong D, Hasanović A, Feliachi A. Robust load frequency control using genetic algorithms and linear matrix inequalities. *IEEE Transactions on Power Systems* 2003; **18**(2):861–885.
22. Bacconi F, Mosca E, Casavola A. Hybrid constrained formation flying control of micro-satellites. *IET Control Theory and Applications* 2007; **1**(2):513–521.
23. Douglas DA, Edris A-A, Pritchard GA. Field application of a dynamic thermal circuit rating method. *IEEE Transactions on Power Delivery* 1997; **12**(2):823–832.
24. Gellings CW. CEIDS and then power delivery system of the future. *CEIDS and the Power Delivery System of the Future Rev. 3.14.03*, 2003.
25. Angeli D, Mosca E. Command governor for nonlinear systems under constraints. *IEEE Transactions on Automatic Control* 1999; **44**:816–820.
26. Angeli D, Casavola A, Mosca E. Command governors for constrained nonlinear systems: direct nonlinear vs linearization-based strategies. *International Journal of Robust and Nonlinear Control* 1999; **9**:677–699.

DOI: 10.1002/acs